Effects of Heat Transfer and Concentration on Peristaltic Ree-Eyring Fluid Flow in a Symmetric Channel with Square and Triangular Boundaries

Fatima K. Abdullah [1], Ahmed M. Abdulhadi [2]

[1]Department of mathematics, college of science, University of Baghdad, Baghdad, Iraq
[2] Department of computer engineering techniques, Dijlah University College, Baghdad, Iraq
f.abdullah@coeng.uobaghdad.edu.iq

Article Info	ABSTRACT

ABSTRACT

This article aims to investigate the effects of heat transfer analysis, Ree-Eyring fluid concentration, magnetic field, porous media, and MHD on the peristaltic transport of Ree-Eyring fluid in a rotating frame within a symmetric channel that experiences triangular and square boundary in three dimensions. The governing equations are written, which are continuity, motion, heat, and concentration equations with help of conservation of mass, Newton's second law, and conservation of energy, respectively. We then simplified the equations using the long wave length hypothesis and the Renold number approximation. This approximation led to the development of nonlinear differential equations. The exact solution of the Ree-Eyring particle concentration, temperature, velocity, and stream function are calculated. Using the MATHMETICA program, we have graphically clarified the flow quantities for different parameters. We have also graphically explained the trapping phenomenon. In this analysis, we observed that highlighting the concentration of fluid leads to a decrease in axial velocity and secondary velocity. The increase in the magnetic field resulted in an increase in axial velocity, but a decrease in secondary velocity. We observed an increase in trapping phenomena as the concentration of fluid increase and it decrease as the magnetic field increase.

Corresponding Author:

Fatima K. Abdullah
Department of mathematics, college of science, University of Baghdad, Baghdad, Iraq
Aljadria, university street, Baghdad, Iraq
Email: f.abdullah@coeng.uobaghdad.edu.iq

1. INTRODUCTION

Numerous articles have addressed the peristalsis of various fluid models and flow configurations [1-7]. If you wish to understand the rheological characteristics of biological fluids such as blood, saliva, intravascular fluids, intracellular fluids, and interstitial fluids, you should study the peristalsis of Ree-Eyring non-Newtonian fluid. The study explores the cross-diffusive magnetohydrodynamic peristaltic transport of a Ree-Eyring fluid, which modifies the activation energy while permitting tiny particles to pass through a flexible porous channel.[8]. In order to

simulate the peristaltic flow of a Ree-Eyring liquid over a uniform, compliant conduit, the effects of variable viscosity and thermal conductivity were investigated in [9]. Understanding viscosity variation is essential to comprehending blood flow in the biological system of the human body because blood in the peripheral region has a lower viscosity than blood in the core region. The viscosity dependency of pressure has been the subject of various papers and investigations over the years. References [10-14] offer a thorough analysis of this subject. The peristaltic process of a non-Newtonian Ree-Eyring liquid is an essential component of medical technology in the face of shifting liquid properties and heat transfer. the method that examined and evaluated the impacts of the wall's properties as well as the liquid's fluctuating characteristics in [15]. Heat transfer analysis and magnetohydrodynamics (MHD) are examined in connection with peristalsis for Ree-Eyring fluid in a rotating frame [16]. The impact of heat transfer analysis, concentration of Ree-Eyring fluid, magnetic field, porous media and (MHD) on peristaltic transport for Ree-Eyring fluid in rotating frame on the three dimensions are studied in [19]. the impact of heat transfer analysis, concentration of Ree-Eyring fluid, magnetic field, porous media, and MHD on peristaltic transport for Ree-Eyring fluid in a rotating frame in an inclined channel with triangular and square boundary on the three dimensions are discussed in [20]. In the current paper we study the impact of heat transfer analysis, magnetic field, porous media, concentration and (MHD) on peristaltic transport of Ree-Eyring fluid in rotating frame. The governing equations are written, which are continuity, motion, heat, and concentration equations with help of conservation of mass, Newton's second law, and conservation of energy, respectively. Then simplified under the hypothesis of the long wave length and the law Renold number approximation. The exact solution of the Ree-Eyring particle concentration, temperature, flow rate, axial velocity, secondary velocity and stream function are calculated by using the perturbation method.

2.   Mathematical model

Assume that a rotating frame used to transport an incompressible MHD Ree-Ering fluid peristaltically through a symmetric channel with the upper wall $\bar{H}_2$ and the lower wall $\bar{H}_1$.. see Figure (1).
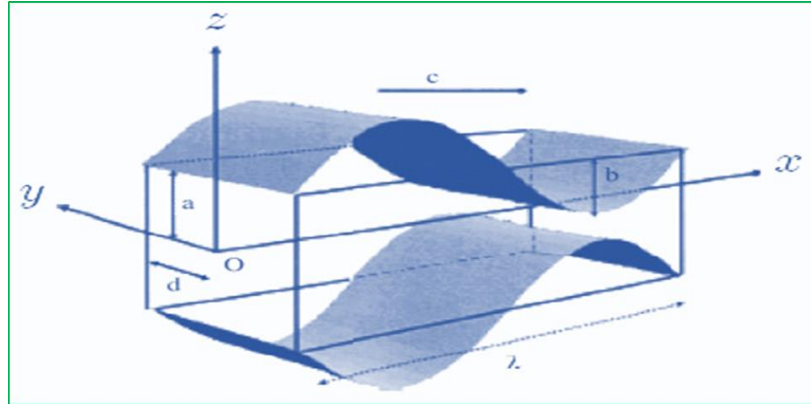.

Figure -1 The problem's geometry

the flow moves at a constant speed of c with varying wave amplitudes, phase. The uniform magnetic field $= (0, \beta_0, 0)$. The equations of boundary are [17]:

$$\bar{Z} = \bar{H}_1(\tilde{x}, \check{t}) = d + \bar{m}\tilde{x} + a\left[\frac{8}{\pi^3}\sum_{n=1}^{\infty}\frac{(-1)^{n+1}\sin\frac{(2\pi(2n-1)(\tilde{x}-c\check{t})}{\lambda}}{(2n-1)^2}\right] \tag{1}$$

$$\bar{Z} = \bar{H}_2(\tilde{x}, \check{t}) = d + \bar{m}\tilde{x} + a\left[\frac{\pi}{4}\sum_{n=1}^{\infty}\frac{(-1)^{n+1}\cos\frac{(2\pi(2n-1)(\tilde{x}-c\check{t})}{\lambda}}{(2n-1)}\right] \tag{2}$$

Where ε represents the wave amplitudes along the wall, the wavelength is λ, the time is t, and m' is the non-uniform parameters where,

$$\tilde{v}_I = (\tilde{u}, \tilde{v}, \tilde{w}) \tag{3}$$
$$\tilde{x}_J = (\tilde{x}, \tilde{y}, \tilde{z}) \tag{4}$$

3.   Governing Equations

The incompressible irrotational laminar flow energy and moment equation, in addition to the governing equations for the fixed frame of continuity, are as follows [18].

$$\frac{\partial \tilde{u}}{\partial \tilde{x}} + \frac{\partial \tilde{w}}{\partial \tilde{z}} = 0 \tag{5}$$

$$\rho \frac{\partial \tilde{u}}{\partial \tilde{t}} - 2\rho\Omega\tilde{v} = -\frac{\partial \bar{P}}{\partial \tilde{x}} + \frac{\partial \tau_{\tilde{x}\tilde{x}}}{\partial \tilde{x}} + \frac{\partial \tau_{\tilde{x}\tilde{y}}}{\partial \tilde{y}} + \frac{\partial \tau_{\tilde{x}\tilde{z}}}{\partial \tilde{z}} - \sigma\beta_0^2\tilde{u} - \frac{\mu}{k_0}\tilde{u} + \rho g\beta_T(T-T_0) + \rho g\beta_C(C-C_0) \tag{6}$$

$$\rho \frac{\partial \tilde{v}}{\partial \tilde{t}} + 2\rho\Omega\tilde{u} = -\frac{\partial \bar{P}}{\partial \tilde{y}} + \frac{\partial \tau_{\tilde{y}\tilde{x}}}{\partial \tilde{x}} + \frac{\partial \tau_{\tilde{y}\tilde{y}}}{\partial \tilde{y}} + \frac{\partial \tau_{\tilde{y}\tilde{z}}}{\partial \tilde{z}} \tag{7}$$

$$\rho \frac{\partial \tilde{w}}{\partial \tilde{t}} = -\frac{\partial \bar{P}}{\partial \tilde{z}} + \frac{\partial \tau_{\tilde{z}\tilde{x}}}{\partial \tilde{x}} + \frac{\partial \tau_{\tilde{z}\tilde{y}}}{\partial \tilde{y}} + \frac{\partial \tau_{\tilde{z}\tilde{z}}}{\partial \tilde{z}} - \sigma\beta_0^2\tilde{w} - \frac{\mu}{k_0}\widetilde{W} \tag{8}$$

$$\frac{\partial C}{\partial \tilde{t}} + \tilde{u}\frac{\partial C}{\partial \tilde{x}} + \tilde{v}\frac{\partial C}{\partial \tilde{y}} + \tilde{w}\frac{\partial C}{\partial \tilde{z}} = D_B\left(\frac{\partial^2 C}{\partial \tilde{x}^2} + \frac{\partial^2 C}{\partial \tilde{y}^2} + \frac{\partial^2 C}{\partial \tilde{z}^2}\right) + \frac{D_T}{T_0}\left(\frac{\partial^2 T}{\partial \tilde{x}^2} + \frac{\partial^2 T}{\partial \tilde{y}^2} + \frac{\partial^2 T}{\partial \tilde{z}^2}\right) \tag{9}$$

$$\rho c_p \frac{\partial T}{\partial \tilde{t}} = K'\left(\frac{\partial^2 T}{\partial \tilde{x}^2} + \frac{\partial^2 T}{\partial \tilde{y}^2} + \frac{\partial^2 T}{\partial \tilde{z}^2}\right) + \tau\{D_B\left(\frac{\partial C}{\partial \tilde{x}}\frac{\partial T}{\partial \tilde{x}} + \frac{\partial C}{\partial \tilde{y}}\frac{\partial T}{\partial \tilde{y}} + \frac{\partial C}{\partial \tilde{z}}\frac{\partial T}{\partial \tilde{z}}\right) + \frac{D_T}{T_0}\left(\left(\frac{\partial T}{\partial \tilde{x}}\right)^2 + \left(\frac{\partial T}{\partial \tilde{y}}\right)^2 + \left(\frac{\partial T}{\partial \tilde{z}}\right)^2\right)\} \tag{10}$$

The accompanying conditions are:

$$\left.\begin{array}{l} \tilde{u}_{\tilde{z}} = 0, \tilde{v}_{\tilde{z}} = 0, \ K'\frac{\partial T}{\partial Z} = 0 \text{ at } Z = \bar{H}_1 \\ \tilde{u} = 0, \tilde{v} = 0, \ K'\frac{\partial T}{\partial \tilde{z}} = -\eta(T-T_0) \text{ at } Z = \bar{H}_2 \end{array}\right\} \tag{11}$$

According to the Ree-Eyring fluid model, the stress tensor is defined as [19].

$$\check{\tau}_{ij} = \mu\frac{\partial \tilde{v}_i}{\partial \tilde{x}_j} + \frac{1}{\beta}sinh^{-1}\left(\frac{1}{c}\frac{\partial \tilde{v}_i}{\partial \tilde{x}_j}\right), since \ sinh^{-1}\tilde{x} \approx \tilde{x} \text{ for } |\tilde{x}| \leq 1 \text{ then,}$$

$$\check{\tau}_{ij} = \mu\frac{\partial \tilde{v}_i}{\partial \tilde{x}_j} + \frac{1}{\beta}(\frac{1}{c}\frac{\partial \tilde{v}_i}{\partial \tilde{x}_j}) \tag{12}$$

The terms ($\bar{P}, \rho, \beta_0, \sigma, k_0, \beta_T, \beta_C, T_0, T, K', c_p, Q_0$ and η) represent the modified pressure, fluid density, the constant magnetic field, the electric conductivity the permeability parameter, the coefficient of linear thermal expansion, the coefficient of linear concentration, temperature at wall, temperature, thermal conductivity, specific heat, the heat conduction and absorption constant and heat transfer coefficient respectively, μ is a fluid`s dynamic viscosity, material constants c and β. Despite the inherent unsteady of peristaltic transport, we can overlook it when we use the change from the wave frame (move frame) $(\bar{x}, \bar{y}. \bar{z})$ to the fixed frame $(\tilde{x}, \tilde{y}, \tilde{z})$, which is defined as [18].

$$\left.\begin{array}{l} \bar{x} = \tilde{x} - c\check{t}, \bar{y} = \tilde{y}, \bar{z} = \tilde{z}, \bar{u}(\bar{x}, \bar{y}, \bar{z}) = \tilde{u}(\tilde{x}, \tilde{y}, \tilde{z}) - c \\ \bar{v}(\bar{x}, \bar{y}, \bar{z}) = \tilde{v}(\tilde{x}, \tilde{y}, \tilde{z}) \ and \ \bar{w}(\bar{x}, \bar{y}, \bar{z}) = \tilde{w}(\tilde{x}, \tilde{y}, \tilde{z}) \end{array}\right\} \tag{13}$$

Now, using equation 13, we translate the equations (1–12) into a wave frame to get:

$$\frac{\partial \bar{u}}{\partial \bar{x}} + \frac{\partial \bar{w}}{\partial \bar{z}} = 0$$
(14)

$$\rho\left((\bar{u} + c)\left(\frac{\partial \bar{u}}{\partial \bar{x}} + \frac{1}{\rho}\left(\sigma\beta_0^2 + \frac{\mu}{k_0}\right)\right) + \bar{v}\frac{\partial \bar{u}}{\partial \bar{y}} + \bar{w}\frac{\partial \bar{u}}{\partial \bar{z}} - 2\Omega\bar{v} - g\beta_T(T-T_0) - g\beta_C(C-C_0)\right)$$
$$= -\frac{\partial \bar{P}}{\partial \bar{x}} + \frac{\partial \tau_{\bar{x}\bar{x}}}{\partial \bar{x}} + \frac{\partial \tau_{\bar{x}\bar{y}}}{\partial \bar{y}} + \frac{\partial \tau_{\bar{x}\bar{z}}}{\partial \bar{z}}$$
(15)

$$\rho\left((\bar{u} + c)\frac{\partial \bar{v}}{\partial \bar{x}} + \bar{v}\frac{\partial \bar{v}}{\partial \bar{y}} + \bar{w}\frac{\partial v}{\partial \bar{z}} + 2\Omega(\bar{u} + c)\right) = -\frac{\partial \bar{P}}{\partial \bar{y}} + \frac{\partial \bar{\tau}_{\bar{y}\bar{x}}}{\partial \bar{x}} + \frac{\partial \tau_{\bar{y}\bar{y}}}{\partial \bar{y}} + \frac{\partial \tau_{\bar{y}\bar{z}}}{\partial \bar{z}}$$
(16)

$$\rho\left((\bar{u} + c)\frac{\partial \bar{w}}{\partial \bar{x}} + \bar{v}\frac{\partial \bar{w}}{\partial \bar{y}} + \bar{w}\frac{\partial \bar{w}}{\partial \bar{z}}\right) = -\frac{\partial \bar{P}}{\partial \bar{z}} + \frac{\partial \tau_{\bar{z}\bar{x}}}{\partial \bar{x}} + \frac{\partial \tau_{\bar{z}\bar{y}}}{\partial \bar{y}} + \frac{\partial \tau_{\bar{z}\bar{z}}}{\partial \bar{z}} - \sigma\beta_0^2\bar{w} - \frac{\mu}{k_0}\bar{w}$$
(17)

$$\frac{\partial C}{\partial \check{t}} + (\bar{u} + c)\frac{\partial C}{\partial \bar{x}} + \bar{v}\frac{\partial C}{\partial \bar{y}} + \bar{w}\frac{\partial C}{\partial \bar{z}} = D_B\left(\frac{\partial^2 C}{\partial \bar{x}^2} + \frac{\partial^2 C}{\partial \bar{y}^2} + \frac{\partial^2 C}{\partial \bar{z}^2}\right) + \frac{D_T}{T_0}\left(\frac{\partial^2 T}{\partial \bar{x}^2} + \frac{\partial^2 T}{\partial \bar{y}^2} + \frac{\partial^2 T}{\partial \bar{z}^2}\right) \tag{18}$$

$$\rho c_p \frac{\partial T}{\partial \check{t}} = K'\left(\frac{\partial^2 T}{\partial \bar{x}^2} + \frac{\partial^2 T}{\partial \bar{y}^2} + \frac{\partial^2 T}{\partial \bar{z}^2}\right) + \tau\{D_B\left(\frac{\partial C}{\partial \bar{x}}\frac{\partial T}{\partial \bar{x}} + \frac{\partial C}{\partial \bar{y}}\frac{\partial T}{\partial \bar{y}} + \frac{\partial C}{\partial \bar{z}}\frac{\partial T}{\partial \bar{z}}\right) + \frac{D_T}{T_0}\left(\left(\frac{\partial T}{\partial \bar{x}}\right)^2 + \left(\frac{\partial T}{\partial \bar{y}}\right)^2 + \left(\frac{\partial T}{\partial \bar{z}}\right)^2\right)\} + Q_0 \tag{19}$$

4. Dimensionless Parameters

The following dimensionless variables and parameters are introduced

$$\omega = \frac{T-T_0}{\Delta \bar{T}}, Re = \frac{cd}{v}, \ \delta = \frac{d}{\lambda}, v = \frac{\mu}{\rho}, Pr = \frac{\mu c_p}{K'}, Gr = \frac{\rho g \beta_T T_0 d^2}{\mu c}, t = \frac{c\bar{t}}{\lambda}$$

$$P = \frac{\bar{P}d^2}{\mu \lambda c}, \alpha = \frac{1}{\mu \beta c}, S = \frac{Q_\circ d^2}{K'T_0}, u = \frac{\bar{u}}{c}, v = \frac{\bar{v}}{c}, w = \frac{\bar{w}}{c}, \ Da = \frac{k_0}{d^2}$$

$$y = \frac{\bar{y}}{\lambda}, x = \frac{\bar{x}}{\lambda}, z = \frac{\bar{z}}{d}, m = \frac{\lambda \bar{m}}{d}, \ H = \sqrt{\frac{\delta}{\mu}} B_\circ d, T1 = \frac{Re\Omega d}{c}$$

$$h_{1,2} = \frac{\bar{H}_{1,2}}{d}, \varepsilon = \frac{a}{d}, M^2 = (H^2 + \frac{1}{Da}), \tau_{ij} = \frac{d\bar{\tau}_{ij}}{\mu c}, \Phi = \frac{C-C_0}{C_1-C_0}$$

$$Br = \frac{\rho g \beta_c (C-C_0)d^2}{\mu c}, \ Nt = \frac{\tau D_T(T-T_0)}{T_0 v}, \ Nb = \frac{\tau D_B(C-C_0)}{v}, Le = \frac{v}{D_B}$$

(20)

Where $Re, Pr, Gr, T1, \alpha, S, v, H, Le, and \ Da$ are the Renold number, Prandtl number, Grashoff number, Taylor number, fluid parameter, heat source/sink parameter, kinematic viscosity, Hartman number, regular Lewis number and Darcy number respectively. The dimensionless stream function $\psi, u = \frac{\partial \psi}{\partial z}$ and $w = -\delta \frac{\partial \psi}{\partial x}$ in equations (14-19) is now introduced, together with the following non-dimensional amounts from (20) we obtain:

$$\frac{\partial P}{\partial x} - \frac{\partial \tau_{xz}}{\partial z} + H^2 \left(\frac{\partial \psi}{\partial z} + 1\right) + \frac{1}{Da}\left(\frac{\partial \psi}{\partial z} + 1\right) - 2T1v - Gr\omega - Br\Phi = 0 \quad (21)$$

$$\frac{\partial P}{\partial y} - \frac{\partial \tau_{yz}}{\partial z} + 2T1\left(\frac{\partial \psi}{\partial z} + 1\right) = 0 \quad (22)$$

$$\frac{\partial P}{\partial z} = 0 \quad (23)$$

$$\frac{\partial^2 \Phi}{\partial z^2} + \frac{Nt}{Nb}\frac{\partial^2 \omega}{\partial z^2} = 0 \quad (24)$$

$$\frac{\partial^2 \omega}{\partial z^2} + PrNb\frac{\partial \Phi}{\partial z}\frac{\partial \omega}{\partial z} + PrNt\left(\frac{\partial \omega}{\partial z}\right)^2 + S = 0 \quad (25)$$

Where

$$\tau_{xz} = (1+\alpha)\frac{\partial^2 \psi}{\partial z^2}, \quad \tau_{yz} = (1+\alpha)\frac{\partial v}{\partial z} \quad (26)$$

The boundary conditions' dimensionless form is:

$$h1(x) = 1 + mx + \varepsilon[\frac{8}{\pi^3}\sum_{n=1}^{5}\frac{(-1)^{n+1}\sin(2\pi(2n-1)x)}{(2n-1)^2}] \quad (27)$$

$$h2(x) = 1 + mx + \varepsilon[\frac{\pi}{4}\sum_{n=1}^{5}\frac{(-1)^{n+1}\cos(2\pi(2n-1)x)}{(2n-1)}] \quad (28)$$

$$\psi = 0, \ \frac{\partial^2 \psi}{\partial z} = 0, \frac{\partial v}{\partial z} = 0, \ \frac{\partial \omega}{\partial z} = 0 \ at \ z = h_1$$
(29)

$$\psi = F1, \ \frac{\partial \psi}{\partial z} = -1, \ v = 0, \ \omega = 0 \ at \ z = h_2 \quad (30)$$

Now, Equations (15-17) give:

$$\frac{\partial}{\partial z}\left[\frac{\partial \tau_{xz}}{\partial z} - (H^2 + \frac{1}{Da})\left(\frac{\partial \psi}{\partial z} + 1\right) + 2T1v + Gr\omega + Br\Phi\right] = 0 \quad (31)$$

$$\frac{\partial \tau_{yz}}{\partial z} - 2T1\left(\frac{\partial \psi}{\partial z} + 1\right) = 0$$
(32)

5. Solution of the problem

The solution of the above nonlinear system of equations (21)- (25) subject to boundary conditions equation (27-31), it is found the solution is given by:

$$\Phi(x,y,z) = -\frac{Nt}{Nb}\left(-\frac{Sz}{A1(x,y)NbPr} - \frac{e^{-A_1 NbPrz}A_3(x,y)}{A1(x,y)NbPr} + A_4(x,y)\right) + A_1(x,y)z + A_2(x,y) \quad (33)$$

$$\theta(x,y,z) = -\frac{Sz}{A_1(x,y)NbPr} - \frac{e^{-A_1(x,y)NbPrz}A_3(x,y)}{A_1(x,y)NbPr} + A_4(x,y) \quad (34)$$

$$\psi(z) = \frac{1}{((h1-h2)Nb^2Pr(1+\alpha)^2\ldots((M^2+\sqrt{M^4-16T1}))}e^{-\frac{z\sqrt{\frac{M^2}{1+\alpha}-\frac{\sqrt{M^4-16T1}}{1+\alpha}}}{\sqrt{2}}}C1 + e^{\frac{z\sqrt{\frac{M^2}{1+\alpha}-\frac{\sqrt{M^4-16T1}}{1+\alpha}}}{\sqrt{2}}}C2 + e^{-\frac{z\sqrt{\frac{M^2}{1+\alpha}+\frac{\sqrt{M^4-16T1}}{1+\alpha}}}{\sqrt{2}}}C3 +$$

$$e^{\frac{z\sqrt{\frac{M^2}{1+\alpha}+\frac{\sqrt{M^4-16T1}}{1+\alpha}}}{\sqrt{2}}}C4 - (64(-A^2Brh1^2Nb^4Pr^3 + \cdots + 16h2^5Nb^2Prz(T1)^2))$$

(35)

$$u(z) = -\frac{C1e^{\frac{z\sqrt{\frac{M^2}{1+\alpha}-\frac{\sqrt{M^4-16T1}}{1+\alpha}}}{\sqrt{2}}}\sqrt{\frac{M^2}{1+\alpha}-\frac{\sqrt{M^4-16T'}}{1+\alpha}}}{\sqrt{2}} + \frac{C2e^{\frac{z\sqrt{\frac{M^2}{1+\alpha}-\frac{\sqrt{M^4-16T1}}{1+\alpha}}}{\sqrt{2}}}\sqrt{\frac{M^2}{1+\alpha}-\frac{\sqrt{M^4-16T1}}{1+\alpha}}}{\sqrt{2}} - \frac{C3e^{-\frac{z\sqrt{\frac{M^2}{1+\alpha}+\frac{\sqrt{M^4-16T1}}{1+\alpha}}}{\sqrt{2}}}\sqrt{\frac{M^2}{1+\alpha}+\frac{\sqrt{M^4-16T1}}{1+\alpha}}}{\sqrt{2}} +$$

$$\frac{C4e^{\frac{z\sqrt{\frac{M^2}{1+\alpha}+\frac{\sqrt{M^4-16T1}}{1+\alpha}}}{\sqrt{2}}}\sqrt{\frac{M^2}{1+\alpha}+\frac{\sqrt{M^4-16T1}}{1+\alpha}}}{\sqrt{2}} + \cdots + 16h2^5Nb^2Pr(T1)^2$$

(36)

$$v(z) = -\left(32Da\,e^{\frac{z\frac{1+Da(H^2+\sqrt{\frac{Da^2(H^4-16T1)}{Da^2(1+\alpha)^2}}}{Da(1+\alpha)}-(1+\alpha))}{\sqrt{2}}} + \cdots + c5 + c6\,z\right)$$

(37)

$$A_1(x,y) = -\frac{1}{h1-h2}$$ (38)

$$A_2(x,y) = \frac{h1}{h1-h2}$$

(39)

$$A_3(x,y) = -(h1-h2)\frac{e^{(-\frac{1}{h1-h2})h1NbPr}S}{NbPr}$$ (40)

$$A_4(x,y) = \frac{e^{\frac{1}{h1-h2}h2NbPr}(e^{-\frac{1}{h1-h2}h1NbPr}-\frac{1}{h1-h2}e^{-\frac{1}{h1-h2}h2NbPr}h2NbPr)S}{(\frac{1}{h1-h2})^2Nb^2Pr^2}$$ (41)

where $C1, C2, C3, C4, C5$ are constants.

6.   Results and Discussion

The analysis of "ω" temperature, "u" velocity, "Φ" Concentration and "Ψ" stream function is determined in this section.

6.1   The Distribution of temperature

Graphic results present how the parameters contributing to the temperature behave. Figure (2) illustrates the various values of Pr, m, S, Nb and ε the impact of the temperature. According to the figures, the temperature distribution behaves in a parabolic manner. The temperature decreases in the left and center of the channel and equals in the end of the right of the channel with an increase of Pr but it is decreases in the left and center of the channel and equals in the end of the right of the channel with an increase of Nb in (a) and (d) of figure (2) respectively. In (b) of figure (2) we noted that the temperature decreased in the left and increased in the right of the channel and equal in the center of it with an increase in m. The temperature increases with an increase S in interval $0.6 < z < 1.8$ in (c) of figure (2). In (e) of figure (2) the temperature increases with an increase in ε.

6.2   The Distribution of Concentration

The simulated experiment results, where Φ represents the concentration of the Ree-Eyring fluid on peristaltic flow.   graphically depict the parameters' behavior. Figure 3 illustrates the impact of applying various values of Pr, m, S, Nb, Nt and ε to the concentration of the Ree-Eyring fluid. The concentration decreases in the left and

center of the channel and equal in the end of the right of the channel with an increase on Pr in (a) of figure (3).The concentration increases in the right side and decreases in the left side and it is equal in the middle of the channel in (b) of figure 3. We observed that the concentration increases in the interval $0.5 < z$ and decreases in the interval $z < 0.5$ with an increase on S and Nt in (c) and (e) of figure 3. In (d) of figure 3 noticed that the concentration decreases in the right side and equal in the left side of the channel with an increase on Nb. The concentration of the fluid increases with an increase on ε in (f) of figure 3.

6.3   The Distribution of Axial Velocity

The simulated experiment results, where u represents the axial velocity u on the peristaltic flow axis, graphically depict the parameters' behavior. Figure 4 illustrates the effects of applying various values of $\alpha, T1, F1, S, H, Da, Nt, Pr, Br$ and Nb to the axial velocity u. It is evident that the velocity distribution exhibits a parabolic pattern. In (a) of figure 4, the velocity decreases and near to zero with an increase of α and Da in (a) and (g) of figure (4) respectively. We noted that the velocity u decreases with an increase on $T1, Nb$ and ε in (b), (i) and (j) of figure 4 respectively. The velocity increases with an increase on $F1$ and H in (c) and (f) of figure 4 respectively. The increase in velocity is small with small with increasing Br and Nt in (d) and (h) of figure 4 respectively. While the decrease in velocity is small with increasing S in (e) of figure 4.

6.4   The Distribution of Secondary Velocity

The simulated experiment results, where v represents the velocity on the peristaltic flow axis, graphically depict the parameters' behavior. Figure 5 illustrates the impact of applying various values of $\alpha, T1, F1, S, H, Da, Nt, Pr, Br$ and Nb to secondary velocity. We observed that the secondary velocity v increases in the right side and left side of the channel while equal in the center of it with an increase on α and H in (a) and (g) of figure (5) respectively. The secondary velocity v decreases in the right side of the channel but it is equal in the left side and center of it with increase on $T1, F1, Br$ and Nt in (b), (c), (d) and (h) respectively. But it is decrease in the left side of the channel and equal in center and right side of the channel with an increase on S in (e) of figure (5). In (i) and (j) of figure (5) we noted that the velocity v increases in the right side of the channel and equal in center and in the left side of it with an increase on Nb and ε respectively.

6.5   The Distribution Velocity

The simulated experiment results, where v represents the velocity on the peristaltic flow axis, graphically depict the parameters' behavior. Figure (6) illustrates the impact of applying various values of $\alpha, T1, Br, F1, S, H, Da, Nt,$ Pr, Nb and ε to velocity v. we observed that the velocity v with respect to axial x decreases with an increase on $\alpha, F1, S$ and Da in (a), (c), (e) and (g) of figure (6) respectively. In (b), (d) and (h) of figure (6) we observed that the velocity increases in the center of channel and it is equal in the start and end of it with increase on $T1, Br$ and Nt respectively. With an increase in H the velocity v increases in (f) of figure (6). The velocity no change with an increase on Nb in (i) of figure (6). In (j) of figure (6) we noted that the velocity increase in the start of the channel and it decreases in the other parts of the channel.

6.6   The Trapping Phenomenon

This section is allocated to discuss the impact of different values $F1,$ $Br,$ $S, H,$ $Da,$ Nb, Nt and ε on the stream function. Contour graphs present the fluid's flow pattern. Figures 7-14 show the streamline patterns of Ree-Eyring fluid under the impact of the different above parameters. In Figures 7,8 and 11 we observed that the volume and number of the bolus increase with an increase in values of $F1,$ Br and Da espectively. While in Figures 10, 13, and 14, we noticed that the size and number of the bolus decreases, and it is heading down with an increase in the values of H, Nb and ε respectively. In figures 9 and 12, we noticed that the volume and the number of boluses do not change with the change of values of S and Nt respectively.
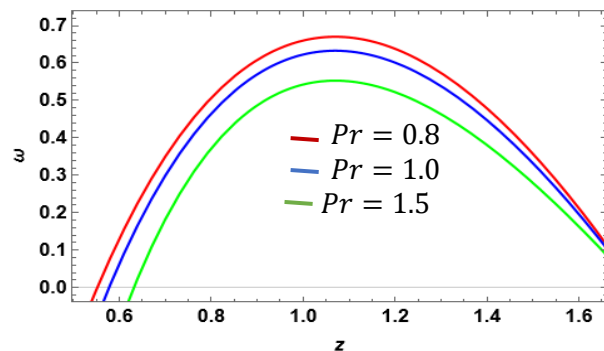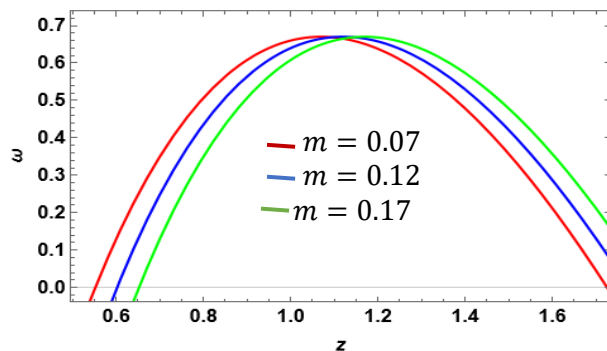
Figure 2: (a) Impact of Pr on tempreture ω

Figure 2: (b) Impact of m on tempreture ω

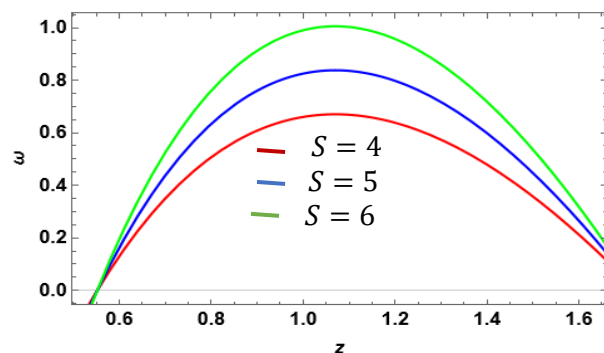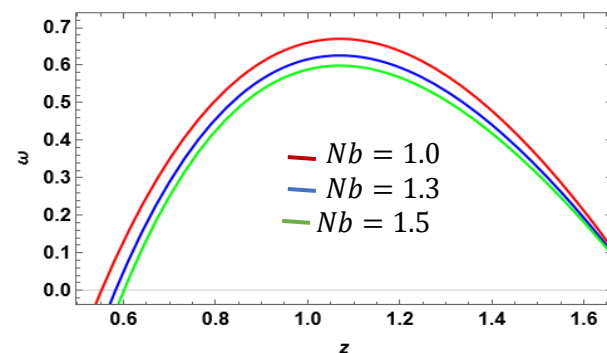Figure 2: (c) Impact of S on tempreture ω
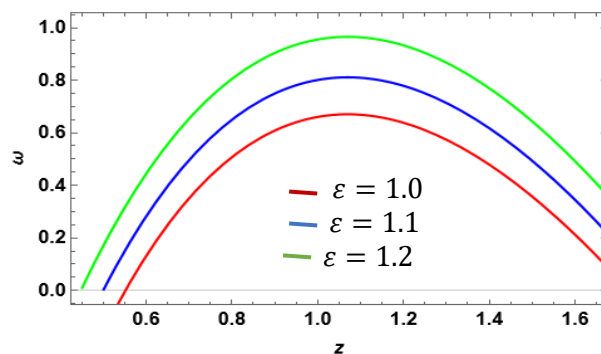
Figure 2: (d) Impact of Nb on tempreture ω

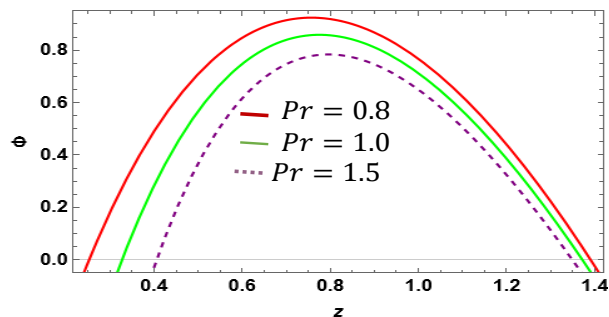Figure 2: (e) Impact of ε on tempreture ω
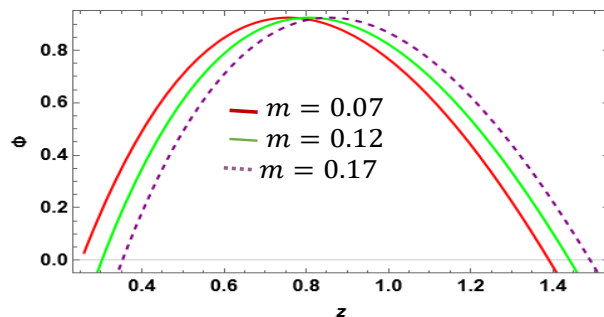
igure 3: (a) Impact of Pr on Concentration Φ
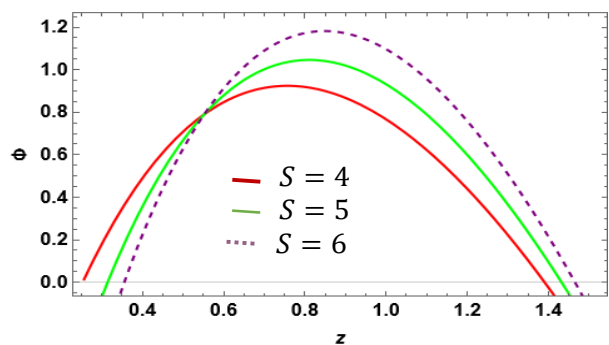

Figure 3: (b) Impact of m on Concentration Φ
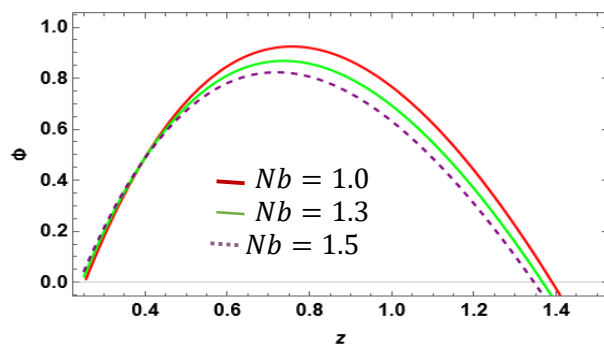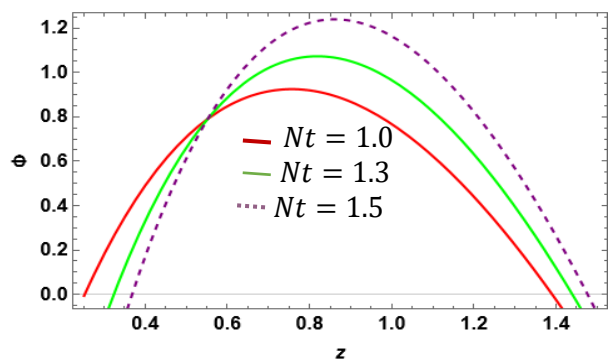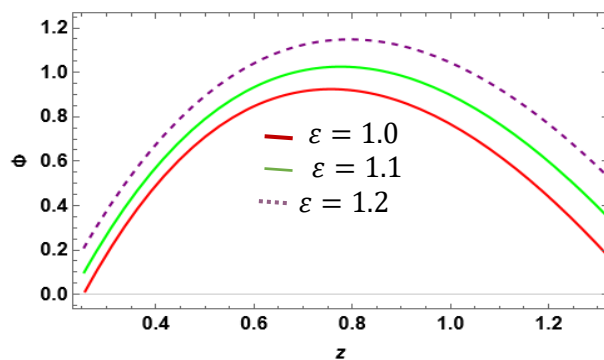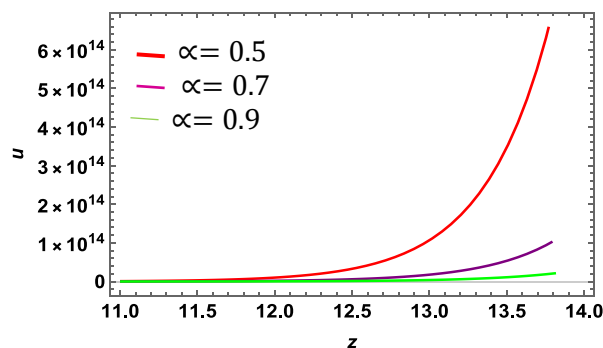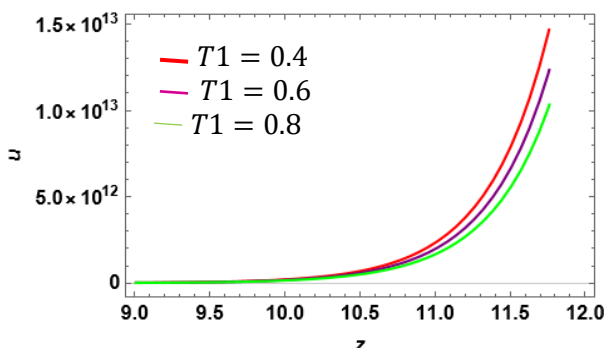

Figure 3: (c) Impact of S on Concentration Φ

Figure 3: (d) Impact of Nb on Concentration Φ

Figure 3: (e) Impact of Nt on Concentration Φ

Figure 3: (f) Impact of ε on Concentration Φ

Figure 4: (a) Impact of $\propto$ on velocity u

Figure 4: (b) Impact of $T1$ on velocity u
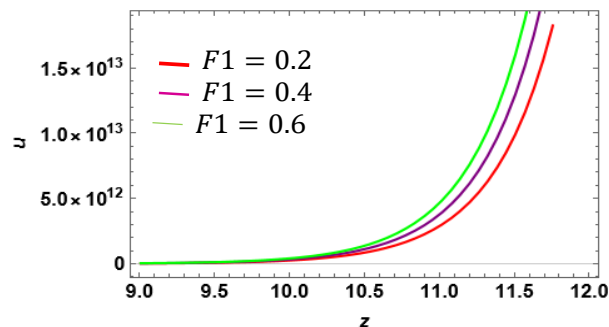
Figure 4: (c) Impact of $F1$ on velocity u
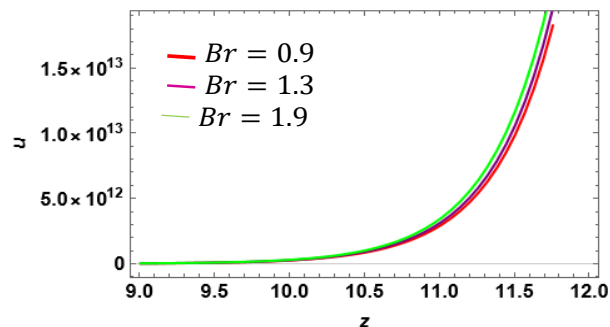
Figure 4: (d) Impact of Br on velocity u
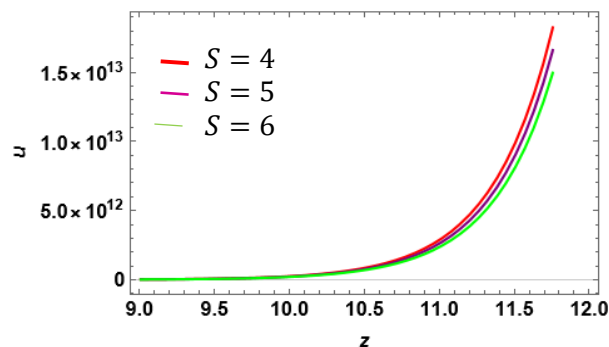
Figure 4: (e) Impact of S on velocity u
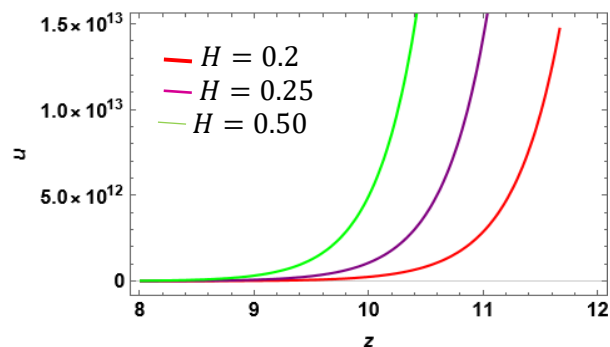
Figure 4: (f) Impact of H on velocity u
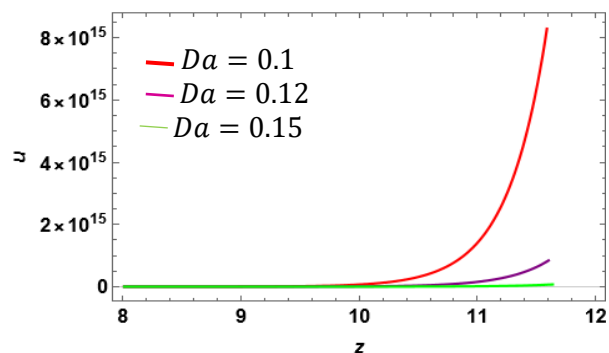
Figure 4: (g) Impact of Da on velocity u
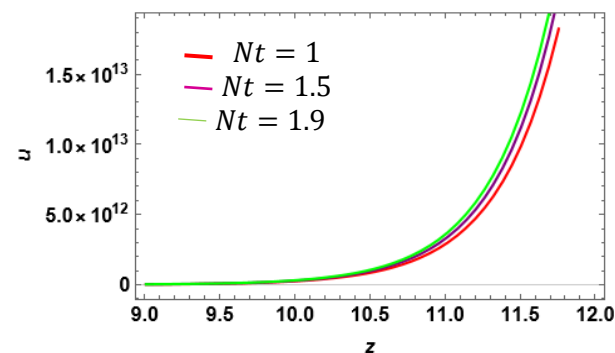
Figure 4: (h) Impact of Nt on velocity u
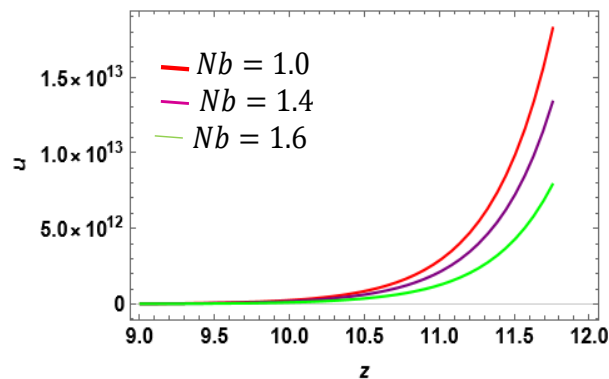
Figure 4: (i) Impact Nb on velocity u
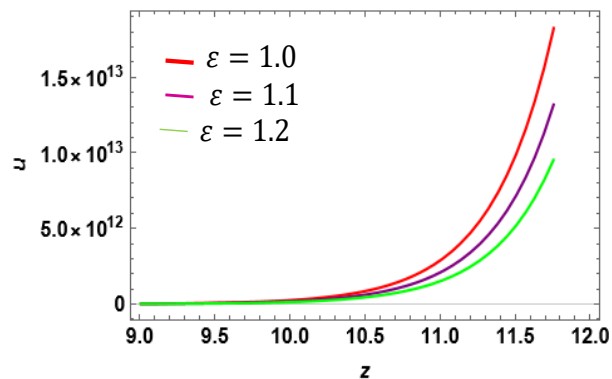
Figure 4: (j) Impact of ε on velocity u
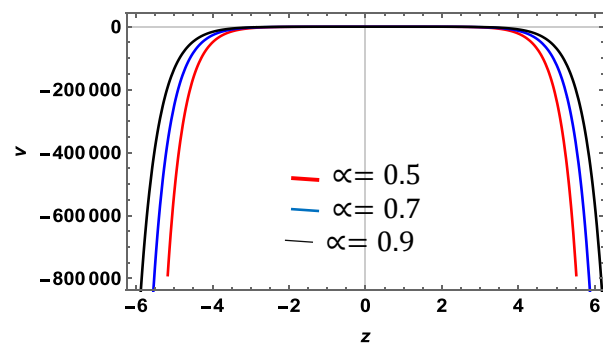
Figure 5: (a) Impact $\propto$ on velocity v
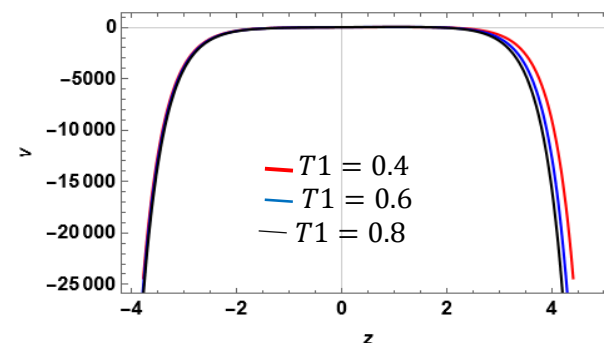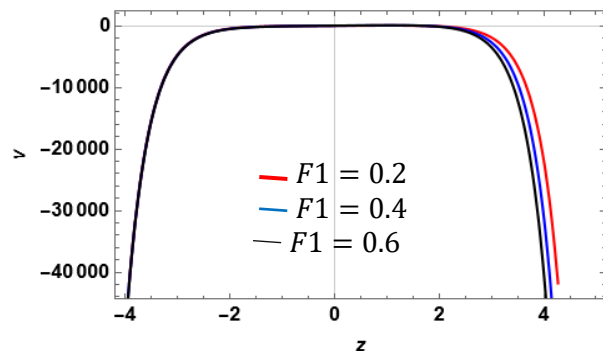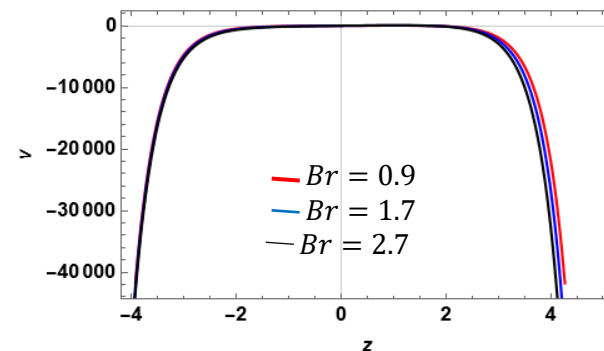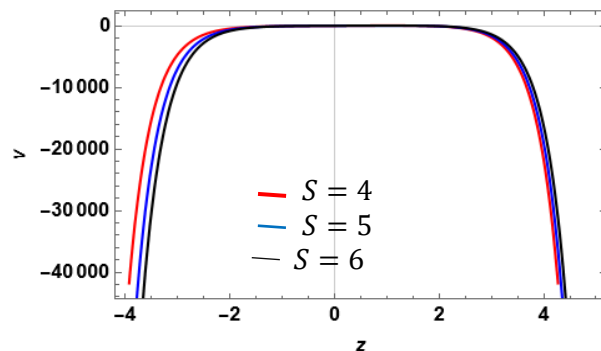
Figure 5: (b) Impact of $T1$ on velocity v

Figure 5: (c) Impact $F1$ on velocity v

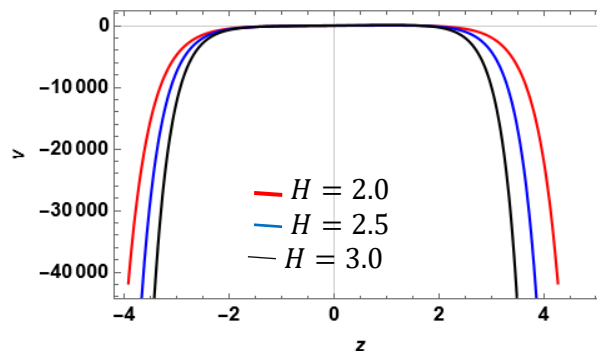Figure 5: (d) Impact of Br on velocity v

Figure 5: (e) Impact S on velocity v

Figure 5: (f) Impact of H on velocity v

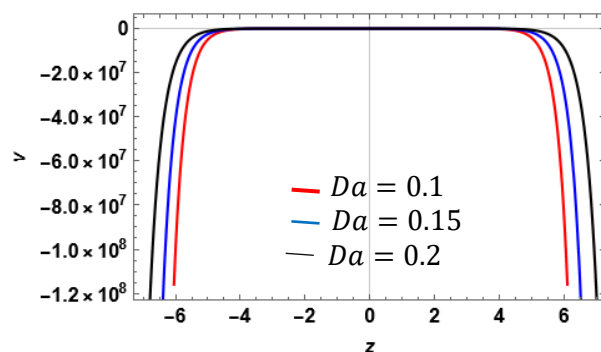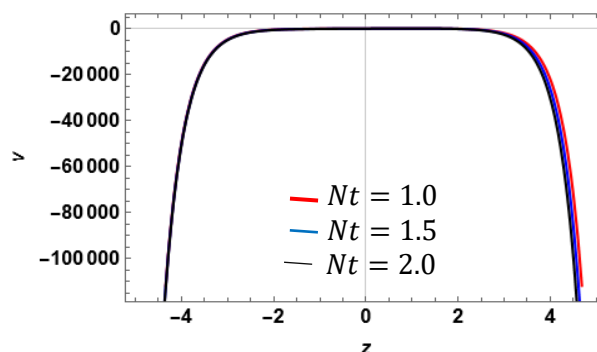Figure 5: (g) Impact Da on velocity v
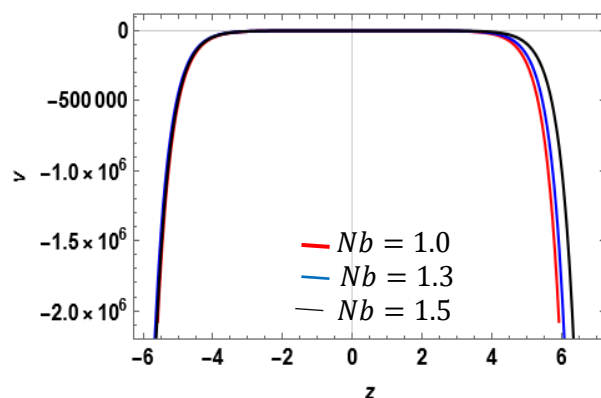
Figure 5: (h) Impact Nt on velocity v
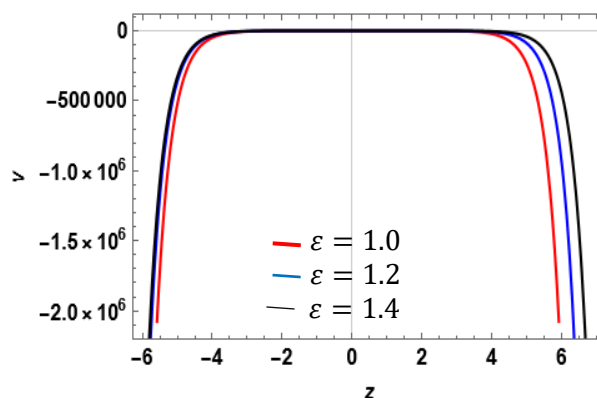
Figure 5: (i) Impact Nb on velocity v

Figure 5: (j) Impact ε on velocity v

Figure 6: (a) Impact $\propto$ on velocity v

Figure 6: (b) Impact $T1$ on velocity v

Figure 6: (c) Impact $F1$ on velocity v

Figure 6: (d) Impact Br on velocity v

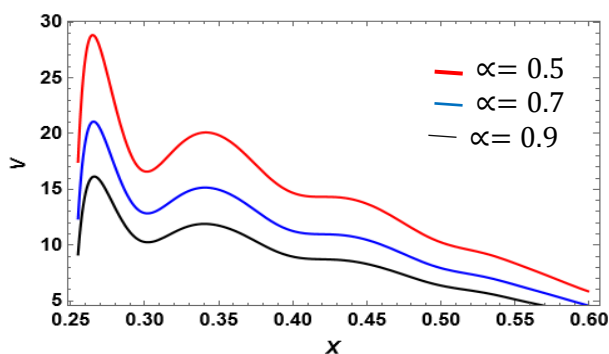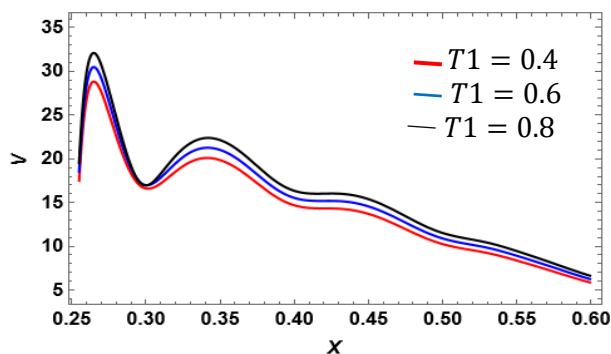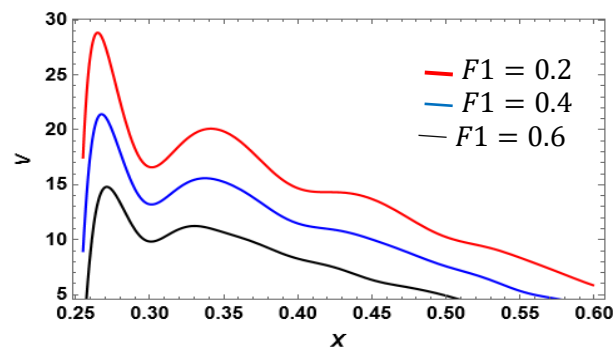Figure 6: (e) Impact S on velocity v
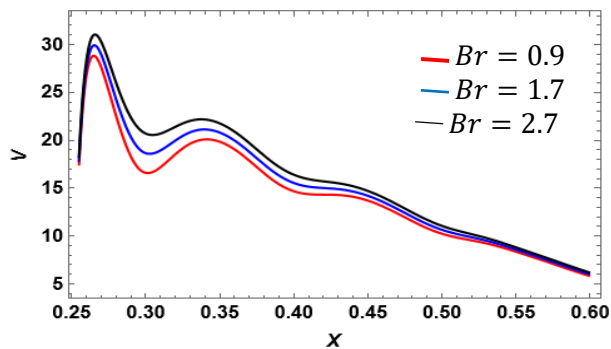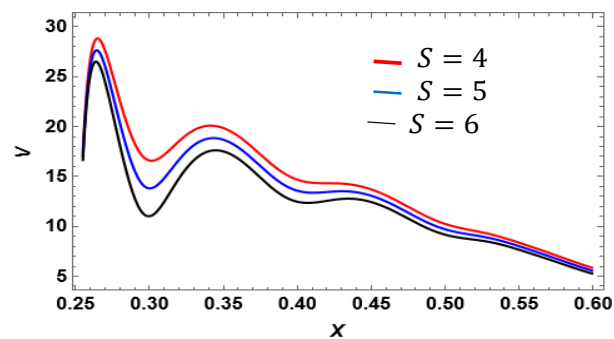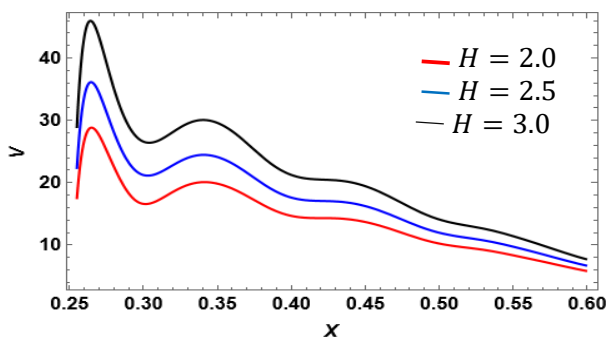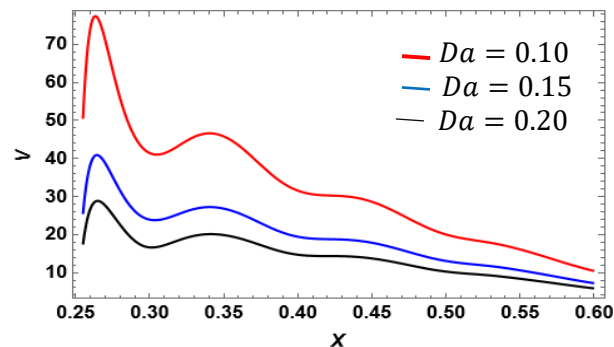
Figure 6: (f) Impact H on velocity v

Figure 6: (g) Impact Da on velocity v

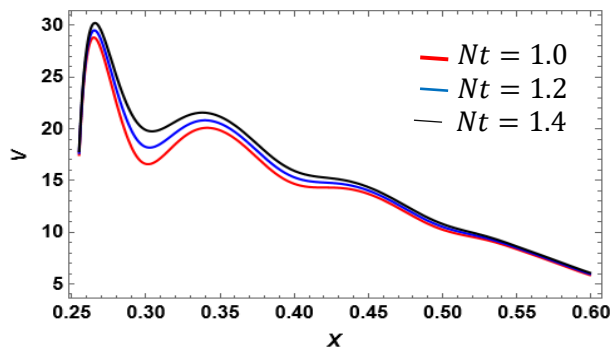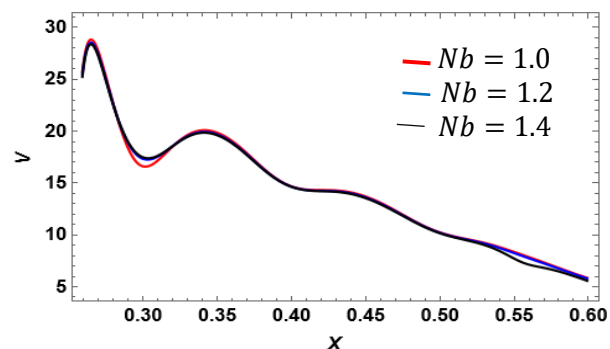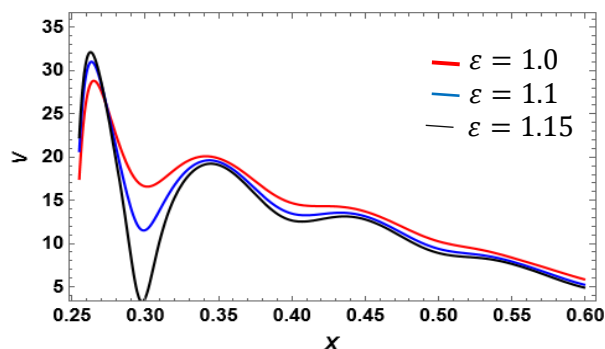Figure 6: (h) Impact Nt on velocity v

Figure 6: (i) Impact Nb on velocity v

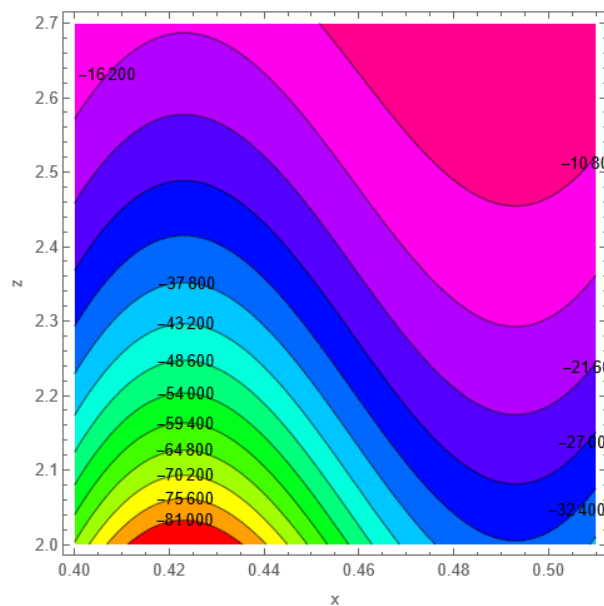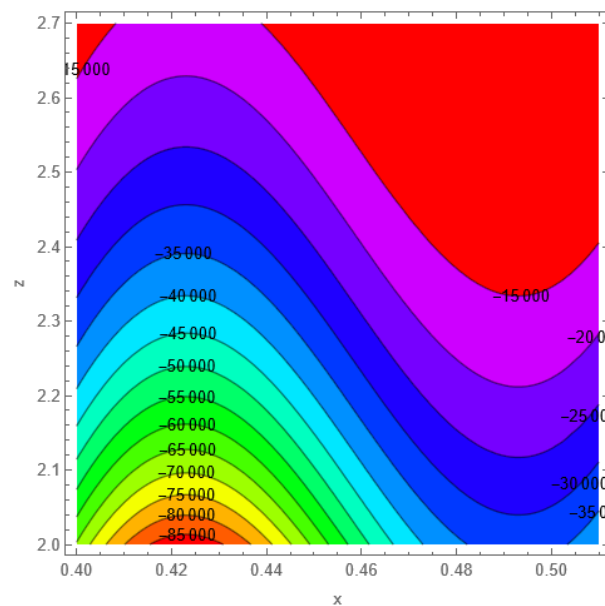Figure 6: (j) Impact ε on velocity v

(a)

(b)

Figure (7): $(a)F1 = 0.2, (b)F1 = 0.6, \alpha = 0.5, T1 = 1.4, Gr = 3, Pr = 0.8, Br = 0.9, 0.07, m = 0.07, S = 4,$
$H = 2, Da = 0.2, Nt = 1, Nb = 1, \varepsilon = 1$

5. conclusion

The effects of heat transfer analysis, Ree-Eyring fluid concentration, magnetic field, porous media, and (MHD) on peristaltic transport for Ree-Eyring fluid in rotating frames in three dimensions are studied in this work. The following is a list of major conclusions:

1. The temperature decreases in the left and center of the channel and equals in the end of the right of the channel with an increase of Pr but it is decreases in the left and center of the channel and equals in the end of the right of the channel with an increase of Nb. we noted that the temperature decreased in the left and increased in the right of the channel and equal in the center of it with an increase in m. The temperature increases with an increase S in interval $0.6 < z < 1.8$. the temperature increases with an increase in ε.

2. The concentration decreases in the left and center of the channel and equal in the end of the right of the channel with an increase on Pr. The concentration increases in the right side and decreases in the left side and it is equal in the middle of the channel. We observed that the concentration increases in the interval $0.5 < z$ and decreases in the interval $z < 0.5$ with an increase on S and Nt. The concentration decreases in the right side and equal in the left side of the channel with an increase on Nb. The concentration of the fluid increases with an increase on .

3. The velocity decreases and near to zero with an increase of α and Da. We noted that the velocity u decreases with an increase on $T1, Nb$ and ε. The velocity increases with an increase on $F1$ and H. The increase in velocity is small with small with increasing Br and Nt. While the decrease in velocity is small with increasing .

4. We observed that the secondary velocity v increases in the right side and left side of the channel while equal in the center of it with an increase on α and H. The secondary velocity v decreases in the right side of the channel but it is equal in the left side and center of it with increase on $T1, F1, Br$ and Nt. But it is decrease in the left side of the channel and equal in center and right side of the channel with an increase on S. We noted that the velocity v increases in the right side of the channel and equal in center and in the left side of it with an increase on Nb and ε.

5. we observed that the velocity v with respect to axial x decreases with an increase on $\alpha, F1,$ S and Da. The velocity increases in the center of channel and it is equal in the start and end of it with increase on $T1, Br$ and Nt. With an increase in H the velocity v increases. The velocity no change with an increase on Nb. We noted that the velocity increase in the start of the channel and it decreases in the other parts of the channel.

6. We observed that the volume and number of the bolus increase with an increase in values of $F1$, Br and Da. While we noticed that the size and number of the bolus decreases, and it is heading down with an increase in the values of H, Nb and ε. The volume and the number of boluses do not change with the change of values of S and Nt.

Refreences

1.   Abdulhussein, H. and A.M. Abdulhadi, *Impact of Couple Stress and Rotation on Peristaltic Transport of a Powell-Eyring Fluid in an Inclined Asymmetric Channel with Hall and Joule Heating.* journal of Basic Sciences, 2022. **8**(13).

2.   Afsar Khan, A., R. Ellahi, and K. Vafai, *Peristaltic transport of a Jeffrey fluid with variable viscosity through a porous medium in an asymmetric channel.* Advances in Mathematical Physics, 2012. **2012**.

3.   Hasona, W., et al., *Combined effects of variable thermal conductivity and electrical conductivity on peristaltic flow of pseudoplastic nanofluid in an inclined non-uniform asymmetric channel: applications to solar collectors.* Journal of Thermal Science and Engineering Applications, 2020. **12**(2): p. 021018.

4.   Jaafar, Z.A., L.Z. Hummady, and M.H. Thawi, *Effects of Rotation and Inclined Magnetic Field on Walters' B Fluid in a Porous Medium using perturbation method or technique.* Iraqi Journal of Science, 2024: p. 818-827.

5.   Ramesh, K. and M. Devakar, *Magnetohydrodynamic peristaltic transport of couple stress fluid through porous medium in an inclined asymmetric channel with heat transfer.* Journal of Magnetism and Magnetic Materials, 2015. **394**: p. 335-348.

6.   Saliha, A.W. and A.M. Abdulhadia, *Properties of Capturing of Peristaltic Flow to A Chemically Reacting Couple Stress Fluid Through an Inclined Asymmetric Channel with Variable Viscosity and Various Boundaries.*

7.   Vaidya, H., et al., *Peristaltic flow of non-Newtonian fluid through an inclined complaint nonlinear tube: application to chyme transport in the gastrointestinal tract.* The European Physical Journal Plus, 2020. **135**(11): p. 1-15.

8.   Ajithkumar, M., P. Lakshminarayana, and K. Vajravelu, *Peristaltic transport of MHD Ree–Eyring fluid through a flexible channel under the influence of activation energy.* Physics of Fluids, 2023. **35**(6).

9.   Rajashekhar, C., et al., *Mass and heat transport impact on the peristaltic flow of a Ree–Eyring liquid through variable properties for hemodynamic flow.* Heat Transfer, 2021. **50**(5): p. 5106-5122.

10.   Abdelsalam, S.I. and M. Sohail, *Numerical approach of variable thermophysical features of dissipated viscous nanofluid comprising gyrotactic micro-organisms.* Pramana, 2020. **94**(1): p. 67.

11.   Abumandour, R.M., et al., *Peristaltic thrusting of a thermal-viscosity nanofluid through a resilient vertical pipe.* Zeitschrift für Naturforschung A, 2020. **75**(8): p. 727-738.

12.   Rajagopal, K., *Couette flows of fluids with pressure dependent viscosity.* International Journal of Applied Mechanics and Engineering, 2004. **9**(3): p. 573-585.

13.   Rajagopal, K., G. Saccomandi, and L. Vergori, *Unsteady flows of fluids with pressure dependent viscosity.* Journal of Mathematical Analysis and Applications, 2013. **404**(2): p. 362-372.

14.   Vaidya, H., et al., *Channel flow of MHD bingham fluid due to peristalsis with multiple chemical reactions: an application to blood flow through narrow arteries.* SN Applied Sciences, 2021. **3**: p. 1-12.

15.   Li, S., et al., *Peristaltic transport of a Ree-Eyring fluid with non-uniform complaint channel: An analysis through varying conditions.* ZAMM-Journal of Applied Mathematics and Mechanics/Zeitschrift für Angewandte Mathematik und Mechanik, 2024. **104**(2): p. e202300073.

16.   Musawi, B.A. and A.M. Abdulhadi. *Influence of heat transfer analysis and (MHD) on peristaltic transport of ree-eyring fluid in rotating frame*. in *AIP Conference Proceedings*. 2023. AIP Publishing.

17.   Hussein, S.A., *Simulating and interpretation of MHD peristaltic transport of dissipated Eyring–Powell nanofluid flow through vertical divergent/nondivergent channel.* Numerical Heat Transfer, Part A: Applications, 2023. 84(10): p. 1124-1148.

18.   Misra, J., B. Mallick, and A. Sinha, *Heat and mass transfer in asymmetric channels during peristaltic transport of an MHD fluid having temperature-dependent properties.* Alexandria engineering journal, 2018. **57**(1): p. 391-406.

19.   Fatima K. Abdullah, Ahmed M. Abdulhadi, *Impact of Concentration and Heat Transfer Analysis on Peristaltic Flow of Ree-Eyring Fluid Under Active of MHD , to publish in the AIP journal of second international conference on advanced research in pure and applied science.*

20*.*   Fatima K. Abdullah, Ahmed M. Abdulhadi, *Impact of Concentration and Heat Transfer   Analysis*

 on Peristaltic Flow of Ree-Eyring Fluid Under Active of MHD in Inclined Channel with Triangular and square boundary, to publish *in the AIP Conference proceedings (ISSN:0094-243X,1551-7616)*

الخلاصة

تهدف هذه المقالة إلى دراسة تأثيرات تحليل انتقال الحرارة وتركيز سائل ري-إيرينج والحقل المغناطيسي والوسائط المسامية والمغناطيسية الديناميكية على النقل التمعجي لسائل ري-إيرينج في إطار دوار داخل قناة متماثلة تواجه حدودًا مثلثية ومربعة في ثلاثة أبعاد. تمت كتابة المعادلات الحاكمة، وهي معادلات الاستمرارية والحركة والحرارة والتركيز بمساعدة قانون الحفاظ على الكتلة وقانون نيوتن الثاني وحفظ الطاقة على التوالي. ثم قمنا بتبسيط المعادلات باستخدام فرضية الطول الموجي الطويل وتقريب رقم رينولد. أدى هذا التقريب إلى تطوير معادلات تفاضلية غير خطية. تم حساب الحل الدقيق لتركيز جسيم ري-إيرينج ودرجة الحرارة والسرعة ودالة التدفق. باستخدام برنامجMATHMETICA ، قمنا بتوضيح كميات التدفق لمعلمات مختلفة بيانياً. لقد شرحنا أيضًا ظاهرة الاحتجاز بيانياً. في هذا التحليل لاحظنا أن إبراز تركيز السائل يؤدي إلى انخفاض في السرعة المحورية والسرعة الثانوية. أدت الزيادة في المجال المغناطيسي إلى زيادة في السرعة المحورية، ولكن إلى انخفاض في السرعة الثانوية. لاحظنا زيادة في ظاهرة الاحتجاز مع زيادة تركيز السائل وانخفاضه مع زيادة المجال المغناطيسي.

96